

Mixing-Controlled Exothermic Fields in Explosions

A. L. Kuhl & R. E. Ferguson¹
Lawrence Livermore National Laboratory
Livermore, CA, USA kuhl2@llnl.gov

A theoretical model of combustion in explosions at large Reynolds, Peclet and Damköhler numbers is described. A key feature of the model is that combustion is treated as material transformations in the Le Chatelier plane, rather than "heat release". In the limit considered here, combustion is concentrated on thin exothermic sheets (boundaries between fuel and oxidizer). The products expand along the sheet, thereby inducing vorticity on either side of the sheet that continues to feed the process. The results illustrate the linking between turbulence (vorticity) and exothermicity (dilatation) in the limit of fast chemistry—thereby demonstrating the controlling role that fluid dynamics plays in such problems.

Formulation

Considered here are mixing-controlled exothermic fields in explosions—as typified by after-burning of TNT explosion products in air. The TNT-air interface is unstable, and rapidly evolves into a turbulent mixing layer. Combustion takes place in the turbulent velocity field of the hot combustion products, so that the oxidation rate is, in effect, controlled by the turbulent mixing rate. The model recognizes three fluids: *fuel-F* (expanded TNT detonation products), *oxidizer-A* (air), and combustion *products-P*. We consider the exothermic-flow limit [5,6] where Reynolds number $Re \gg 1$, Peclet number $Pe \gg 1$, Damköhler number $Da \gg 1$, and Mach number $Ma > 0$. In this limit, effects of molecular transport are negligible (and can therefore be modeled as sub-grid processes). As is typical of combustion in unmixed systems, the fuel reacts with the oxidizer in stoichiometric proportions.

Conservation

In the limit of $Re \gg 1$, the mixture, m , obeys the gas dynamic conservation laws :

Mass: $\partial_t \rho_m + \nabla \cdot (\rho_m \mathbf{u}) = 0$ (1)

Momentum: $\partial_t \rho_m \mathbf{u} + \nabla \cdot (\rho_m \mathbf{u} \mathbf{u}) = - \nabla p_m$ (2)

Energy: $\partial_t \rho_m (u_m + \mathbf{u} \cdot \mathbf{u} / 2) + \nabla \cdot (\rho_m (u_m + \mathbf{u} \cdot \mathbf{u} / 2) \mathbf{u}) = - \nabla \cdot (p_m \mathbf{u})$ (3)

where ρ, u, p and \mathbf{u} denote the density, specific internal energy, pressure and velocity, respectively. These are supplemented by auxiliary balance laws for mass and energy to follow the evolution of the thermodynamic variables of each fluid throughout the domain. In the limit $Pe \gg 1$, the mass balance equations for the fluids acquire the form:

Fuel: $\partial_t \rho_F + \nabla \cdot (\rho_F \mathbf{u}) = -\dot{\rho}_s$ (4)

Air: $\partial_t \rho_A + \nabla \cdot (\rho_A \mathbf{u}) = -\sigma \dot{\rho}_s$ (5)

Products: $\partial_t \rho_P + \nabla \cdot (\rho_P \mathbf{u}) = (1 + \sigma) \dot{\rho}_s$ (6)

where σ denotes the stoichiometric coefficient ($\sigma = 3.2$ for TNT-air). These equations contain source/sink terms that sum to zero—thereby reproducing the mass conservation relation (1) for the mixture. In the limit $Pe \gg 1$, the energy balance equations for the fluids become:

Fuel: $\partial_t \rho_F u_F + \nabla \cdot (\rho_F u_F \mathbf{u}) = -p_F \nabla \cdot \mathbf{u} - u_F \dot{\rho}_s$ (7)

Air: $\partial_t \rho_A u_A + \nabla \cdot (\rho_A u_A \mathbf{u}) = -p_A \nabla \cdot \mathbf{u} - u_A \sigma \dot{\rho}_s$ (8)

Products: $\partial_t \rho_P u_P + \nabla \cdot (\rho_P u_P \mathbf{u}) = -p_P \nabla \cdot \mathbf{u} + u_P (1 + \sigma) \dot{\rho}_s$ (9)

These equations contain source/sink terms that sum to zero, consistent with energy conservation for the mixture (3). Combustion influences these fields through the source $\dot{\rho}_s$.

¹ Krispin Technologies Inc., Rockville, MD

Source

Combustion occurs at the *exothermic surface*: $\mathbf{x}_s(t)$ — which acts simultaneously as a *sink* for F & A and a *source* for P . In the limit of $Da \rightarrow \infty$, the exothermic surface becomes infinitely thin, and may be represented by a Dirac delta function, δ ; its strength satisfies the stoichiometric consumption rule:

$$\dot{\rho}_s(\mathbf{x}, t) = \begin{cases} \rho_F(\mathbf{x}, t)\delta(t - t_s) & (1 - \lambda < 0) \\ \rho_A(\mathbf{x}, t)\delta(t - t_s)/\sigma & (0 < \lambda < 1) \end{cases} \quad (10)$$

where t_s denotes the time when the fluid particle passes through the exothermic surface, while $\lambda(\mathbf{x}, t) = [\text{Air - Fuel ratio}]/\sigma$. The meaning of this notation is:

$$\dot{\rho}_s dV dt = \begin{cases} m_F/\delta V & (1 - \lambda < 0) \\ m_A/(\sigma\delta V) & (0 < \lambda < 1) \end{cases} \quad (11)$$

Thermodynamic Properties

Following [7], the thermodynamic properties of the fluids are represented as loci of states in the Le Chatelier diagram of specific internal energy: u_K as a function of the thermodynamic parameter: $w_K = p_K v_K$ ($K = F, A, R, \& P$), as depicted in Fig. 1. The air curve, A , is based on Gilmore [4]. The fuel curve, F , is based on CHEETAH calculations for TNT [3]. Air and fuel mix to form reactants R according to the stoichiometric rule:

$$u_R = (u_F + \sigma u_A)/(1 + \sigma) \quad \& \quad w_R = (w_F + \sigma w_A)/(1 + \sigma) \quad (12)$$

Starting with points on R , the STANJAN code [8] was used to calculate corresponding thermodynamic equilibrium points on the products curve P . In particular, point i on R transforms to point hp on P for combustion at constant enthalpy & pressure, or to point uv on P for combustion at constant energy & volume. These curves were fit with linear functions:

$$u_A = -0.31909 + 2.65352 w_A \quad \& \quad u_F = -5.28788 + 4.1405 w_F \quad (13)$$

$$u_R = -1.51278 + 2.98856 w_R \quad \& \quad u_P = -4.82385 + 5.40184 w_P \quad (14)$$

where $[u], [w] = \text{kJ/g}$. The above suggest the following form for the equations of state (EOS):

$$u_K = F_K(w_K) - |q_K| + C_K w_K \quad (15)$$

Function F_K represents the general curve of Fig. 1; it is well approximated by the linear relation (15) in the domain of interest; its inverse: $F_K^{-1}(u_K)$ allows one to evaluate w_K from its specific internal energy u_K . Thus, the pressure in a pure fluid K becomes:

$$p_K = \rho_K w_K = \rho_K [u_K + |q_K|]/C_K \quad (16)$$

while for a multi-fluid cell, the mixture pressure is

$$p_m = \rho_m w_m = \rho_m [u_m + |q_m|]/C_m \quad (17)$$

which is based on the mixture properties:

$$\rho_m = \frac{\rho_K}{K}, \quad \rho_m w_m = \frac{\rho_K w_K}{K}, \quad \rho_m u_m = \frac{\rho_K u_K}{K}, \quad \rho_m C_m = \frac{\rho_K C_K w_K / w_m}{K}, \quad \rho_m q_m = \frac{\rho_K q_K}{K} \quad (18)$$

Combustion

The exothermic source was formulated to model confined combustion. It consisted of three sub-grid processes: (i) *reactants formation*: fuel and air molecularly mix in stoichiometric proportions (12) to form reactants (thus modeling sub-grid mass diffusion); (ii) *transformation in the Le Chatelier plane*: reactants are transformed into products at constant uv (for closed systems) or at constant hp (for deflagrations); (iii) *thermal equilibration*: between post-combustion fluids in the cell (thereby mimicking heat diffusion).

Application

The model was used to simulate the explosion of a 0.875-kg cylindrical TNT charge in a 16.6-m^3 chamber. The gas dynamic conservation equations for the mixture (1)-(3) were integrated by means of a higher-order Godunov scheme [2], while the auxiliary mass and energy balance equations (4)-(9) of the fluids were advanced as convection equations based on the same scheme. Adaptive Mesh Refinement [1] was used to follow the mixing on the grid.

Results

A cross-sectional view of the flow field at 2 ms and 5 ms is presented in Fig. 2. Material fields are visualized as *yellow* fuel, *blue* air and *red* combustion products. Velocity fields are visualized by means of vorticity contours (*turquoise*=positive & *chartreuse*=negative) and dilatation contours (*black*=negative). Exothermic cells are marked by *white* stars. Expansion of the TNT products drives a cylindrical blast wave that reflects off the side wall ($r = 117\text{cm}$), and then the end wall ($z = 193\text{cm}$). Fuel consumption takes more than 20 ms.

Blowups of the flow fields are shown in Fig. 3. They focus on one of the large-scale structures near the chamber wall. The exothermic surface is found on the boundary between the *orange* (fuel-rich) products and the *blue* air. Close inspection reveals that the exothermic surface seems to be sandwiched between vortex sheets of opposite sign. This gives the impression that the products expand preferentially along the exothermic surface rather than normal to it (as in a flame), thereby inducing vorticity on both sides of the surface—forming, in effect, an *exothermic doublet sheet*. This impression is confirmed by plots of positive dilatation contours (not shown). These vortex sheets supply the surface with fuel from one side and oxidizer from the other via local entrainment—thereby enhancing the burning rate. By 5 ms, large-scale structures have caused air to be entrained deep within the mixing layer—resulting in numerous folds in the exothermic surface—leading to a more distributed mode of combustion. Weak (acoustic) shock waves (*black* contours) continually wash over the structures.

Conclusions

According to the present Model, combustion consists of material transformations in the Le Chatelier plane—thereby replacing the concept of "heat release". In fact, heat is not released; instead, combustion simply re-arranges the masses and energies among the fluids in an exothermic cell—under the constraint of mass and energy conservation for the mixture.

Numerical simulations based on this Model reveal the characteristics of non-premixed combustion in confined explosions at large Reynolds numbers. In this case, exothermic fields are controlled by turbulent mixing rather than by molecular diffusion. Visualization of the flow field suggests that combustion occurs in thin exothermic sheets. The Model presented here illustrates the link between turbulence (vorticity) and exothermicity (dilatation) in the limit of fast chemistry—thereby demonstrating the controlling role that fluid dynamics plays in such flows.

References

- [1] Berger, M. J. and Colella, P., *J. Comp. Physics*, **82** (1), 1989, pp. 64-84.
- [2] Colella, P. and Glaz, H. M., *J. Comp. Physics*, **59** (2), 1985, pp. 264-289.
- [3] Fried, L. E., *CHEETAH 1.22 User's Manual*, UCRL-MA-117541 (rev. 2), LLNL, 187 pp., 1995.
- [4] Gilmore, F., *Equilibrium Composition and Thermodynamic Properties of Air to 24000 K*, RM-1543, Rand, 1955.
- [5] Kuhl, A. L., & Oppenheim, A.K., "Turbulent Combustion in the Self-Similar Exothermic-Flow Limit", *Advanced Computation and Analysis of Combustion*, ENAS Publishers, Moscow, 1997, pp. 388-396.
- [6] Kuhl, A. L., Ferguson, R. E., & Oppenheim, A. K. "Gasdynamics of Combustion of TNT Products in Air", *Archivum Combustionis*, **19**(1-4), pp. 67-89, 1999.
- [7] Kuhl, A.L., Oppenheim, A.K., Ferguson, R.E., "Thermodynamics of Combustion in a Confined Explosion", *12th All-Union Symposium on Combustion & Explosion*, **1**, pp. 182-184, Inst. Problems of Chemical Physics, 2000.
- [8] Reynolds, W.C., 'STANJAN' *Interactive Programs for Chemical Equilibrium Analysis*, Stanford, 48 p, 1986.

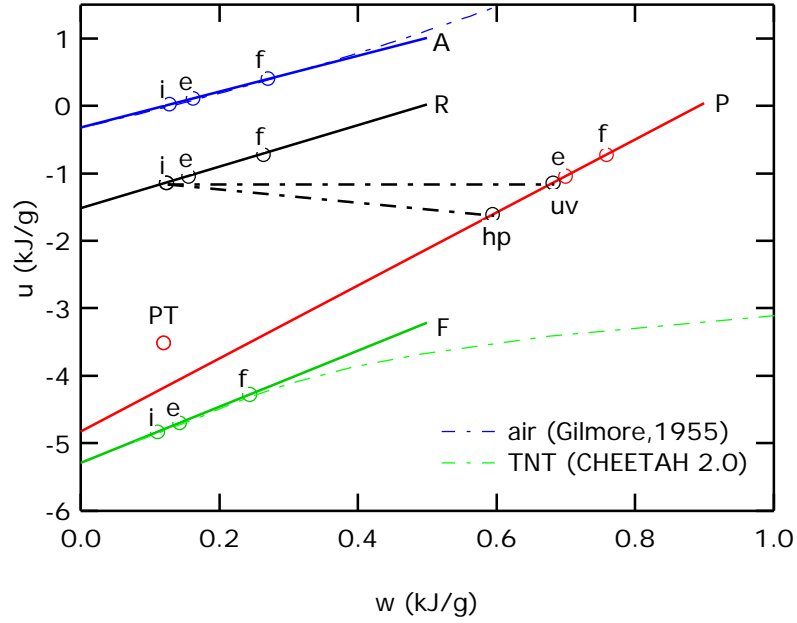


Figure 1. Le Chatelier diagram of states for combustion of Fuel-F (expanded TNT detonation products) with Air-A, forming stoichiometric Reactants-R, which transform into equilibrium combustion products-P.

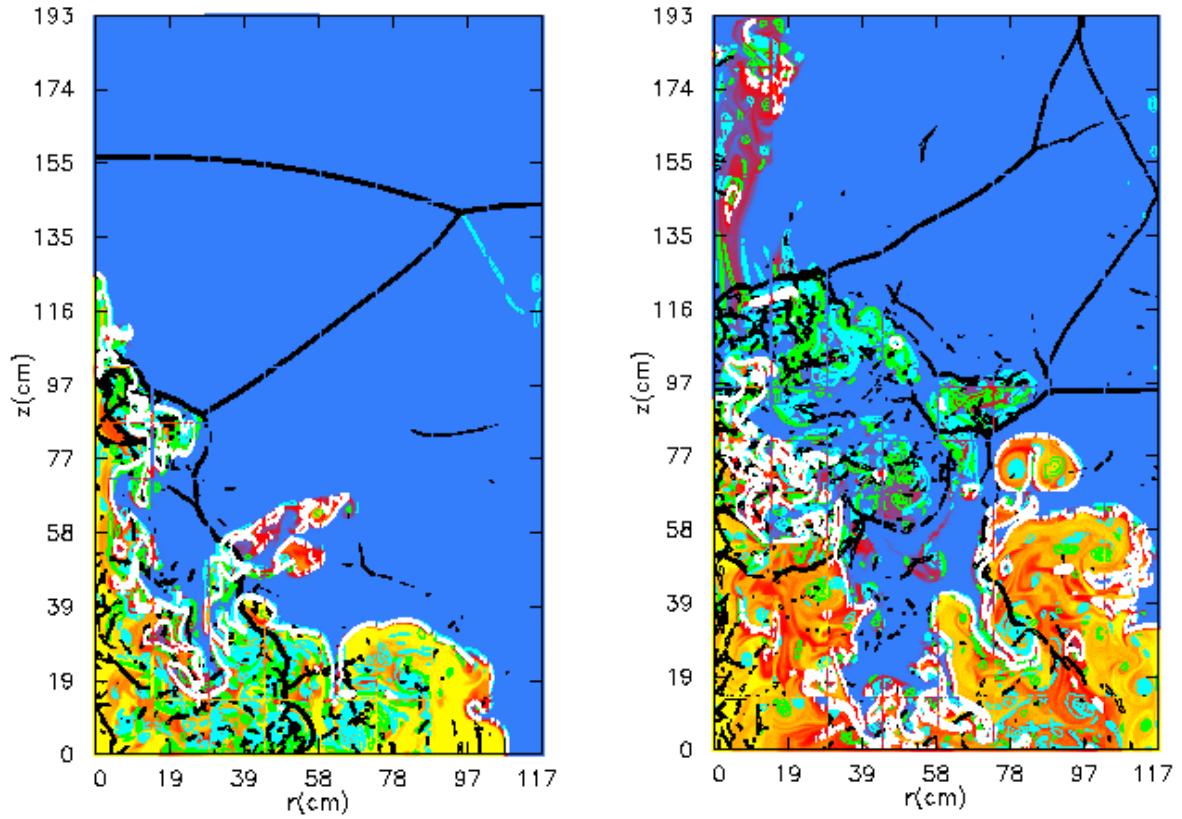


Figure 2. Overall view of the flow field at 2ms and 5ms (for notation, see caption of Fig. 3).

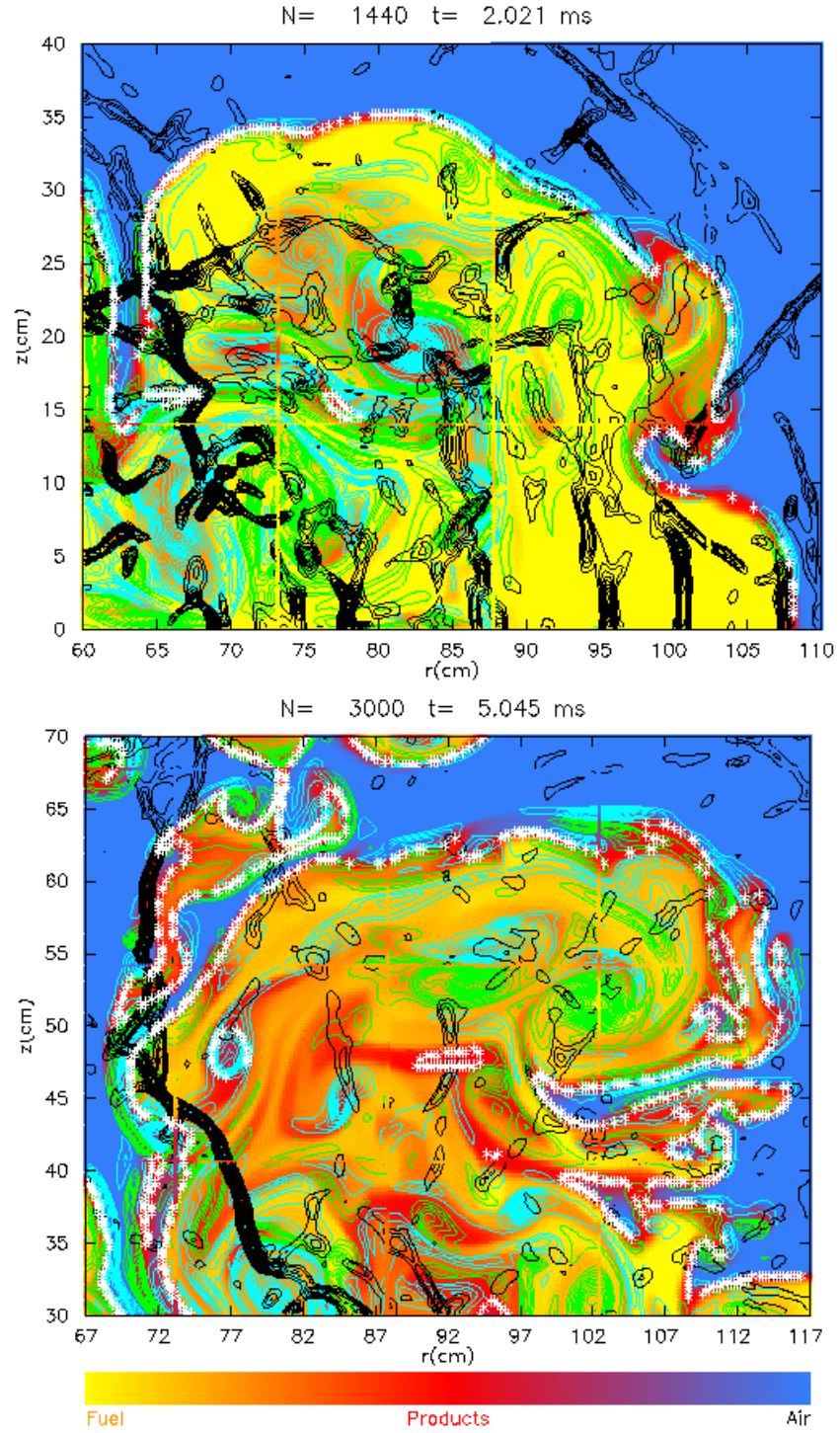


Figure 3. Blow-ups of the flow field created by the explosion of a 1-kg TNT cylinder in a 16.6-m³ chamber at 2 ms and 5 ms. TNT products (shown in yellow) mix with air (depicted as blue) forming combustion products (represented as red). Exothermic cells are marked by white stars. Vorticity contours are turquoise (positive) & chartreuse (negative), while negative dilatation contours are black.